Managing Sustainable Development by Land Cover Prediction Accuracy using Redefined State Transition Matrices in Cellular Automata Markov Chains

Susanta Kundu[1a*], Vinod Kumar [1b], Sugandha Singh [1c]

[1] Faculty of Engineering and Technology, SGT University, Gurgaon, India 122005

[a] susanto.kundu@gmail.com, [b] gvkssun@gmail.com, [c] dean.feat@sgtuniversity.org

ABSTRACT

Sustainable management of agricultural land, forests, urban areas, and water bodies can prevent resource depletion to control environmental degradation. Effective management of agricultural lands, forests, urban areas, and water bodies is critical for preventing resource depletion and mitigating environmental degradation. Accurate land cover predictions over a 30-year period can help policymakers prevent resource depletion and promote sustainability.

This study analyzed historical data for LC classification and then used the Cellular Automata Markov Chain (CA-MC) model to predict future trends. Model reliability is assessed by metrics such as the Kappa coefficient, overall accuracy, user accuracy, and producer accuracy. These metrics measure the agreement between predicted and actual outcomes. With an overall model accuracy of 81.33%, these refinements contribute to the decision-making of policymakers to plan sustainable land use, allocate resources, and balance environmental conservation with economic development. The model supports stakeholders in identifying LC patterns, particularly in urban expansion and deforestation, to promote equitable and sustainable growth.

Keywords: *Urbanization; CA MC; State Transition Matrix; Accuracy, Kappa; Sustainability*

INTRODUCTION

Accuracy improvement in Land Cover (LC) classification for changes provides tangible benefits in long-term planning to balance economic growth, social equity, and environmental conservation. Predicting changes after thirty years provides input for urban planning and informed decision-making. The projected model captures clustered land, forest, urban, and water bodies as the impactful classifications (Memarian *et al.,* 2012), (S. Singh & Biswas, 2022). Historical land data for thirty years is trained to estimate future changes and promote community engagement as an alternative conservation strategy (Subedi *et al.,* 2013). The CA-MC model predicts LC changes stochastically, where the current state(t) is based on the system's previous temporal state(t-1). At its core, a State Transition Matrix (STM), derived from the confusion matrix, forecasts LC changes based on observed data (Mondal *et al.,* 2016). Its elements represent the probability

of LC pixels either remaining in the same class or transforming to another class designated by the cluster dynamics (Arsanjani *et al.,* 2011). The model accuracy influences the effectiveness of policy development to balance economic activities and mitigate the impacts of climate change.

The literature survey reviewed various LC models whose accuracy depends on input data, model configurations, and interpretation of the STM elements. The review finds a gap in realistic interpretations of non-diagonal elements of STM, as most studies focused only on the diagonal elements (treating TRUE) to assess the accuracy. This study fills the gap by redefining some non-diagonal elements of the STM as valid (TRUE) land transitions. For example, transitions from forest to urban or forest to agricultural land are feasible. Similarly, changes from land to urban or land to water bodies are realistic. These inclusions enhance the model's accuracy to help policymakers to plan decisively. Thus, the study bridges futuristic land management using the CA-MC model to improve precision in change predictions. The goal is to redefine some of the non-diagonal elements of the STM to improve accuracy.

MATERIALS AND METHODS

The study explores the spatial-temporal land changes categorized into (1) land, (2) urban, (3) forest, and (4) water bodies. These four categories capture the essential components of the Earth's surface that directly influence ecological balance and serve as sustainability indicators (Qiu *et al.,* 2023). Land represents open land, agricultural fields, crops, sowing areas, or other land

types important for studying soil health. Forests reflect biodiversity and carbon sinks, essential for assessing deforestation, reforestation, and carbon sequestration trends. Urban areas highlight population and infrastructure growth, driving energy demands and resource consumption. Water Bodies encompass lakes, rivers, wetlands, and reservoirs for freshwater availability, flood control, and aquatic ecosystem health. The study reinforces the global relevance of predictive modeling and accuracy assessment. Policymakers can leverage the proposed accuracy refinement to make data-driven decisions, mitigating rapid urban spread and preserving forest areas or agricultural land.

LC Classification

Unsupervised classification k-means was performed on the study area for k=30. Later, it was reclassified into (1) Land (LAN), (2) Forest (FOR), (3) Urban (URB), and (4) Water (WAT) bodies. LAN includes agriculture, crop areas, land waiting for sowing, temporary empty areas, etc., to encompass diverse land types, (2) FOR broadly covers natural forests, cultivated plantations, managed horticulture areas, etc. These are approximately higher than 5m, with a canopy of 10% reaching these dimensions (FAO, 2016). (3) URB is built-up areas including residential, industrial, and factory sheds, roads, etc., and (4) WAT includes rivers, lakes, canals, and natural or artificial reservoirs. These four categories influence ecological balance and serve as sustainability indicators. Their changes in 1993 and 2023 are the basis of training the model. LC changes projected for 2053 using

this model offer future insights into urbanization, water body patterns, and changes in land and forest.

LC Prediction

Leveraging historical data and probabilistic rules, the prediction model captures LC transformations outlined by the CA-MC model. The equation defining the Cellular Automata (CA) model used in this study is

C(t,t+1) = R(C(t),n), where:

C = discrete cellular states, n = number of cellular classifications, t, and t + 1 = two consecutive independent time instants, and R = transformation rule of cellular state changes (Tokihiro *et al.,* 1996).

The Markov Chain predicts LC changes based on the Bayes conditional probability equation given by C(t + 1) = P_{ij} * C(t) where C(t), and C(t + 1) are the two independent system for time = t and (t + 1) states, P_{ij} = state transition matrix calculated by,

$$P_{ij} = \begin{bmatrix} P_{11} & \cdots & P_{1n} \\ \vdots & \vdots & \vdots \\ P_{n1} & \cdots & P_{nn} \end{bmatrix}, where \sum_{j=i}^{n} (P_{ij}) = 1 \; ; \; i$$

and j are LU types.

Each element in the transition matrix P_{ij} has a value between 0 and 1, indicating the state change transition probabilities (Pontius & Schneider, 2001). The transition of a cell state examines the spatial relationships with adjoining cells to update its state (Koomen & Borsboom van Beurden, 2011). In this framework, neighborhood pixels are external factors influencing the state transitions of a pixel (Hamad *et al.,* 2018). The model generates a transition matrix and a change map using Artificial Neural Network (ANN) that simulates a map for 2053, using the 1993-2023 changes as a reference (Markham *et al.,* 2014).

Accuracy Assessment

The overall accuracy assessment measures the agreement between observed and chance classifications, expressed by K = [P(a) − P(e)] / [1 − P(e)], where P(a) is the probability of correctly observed classified image pixel, and P(e) is the probability of predicting a classified image pixel (Mary L. McHugh, 2012). K, the Kappa Coefficient quantifies the accuracy of classifications by comparing observed variables with predicted classifications.

Data Collection

Gurgaon district in Haryana - India, was selected for this study due to its rapid transformation from an agricultural region to an urbanized hub.
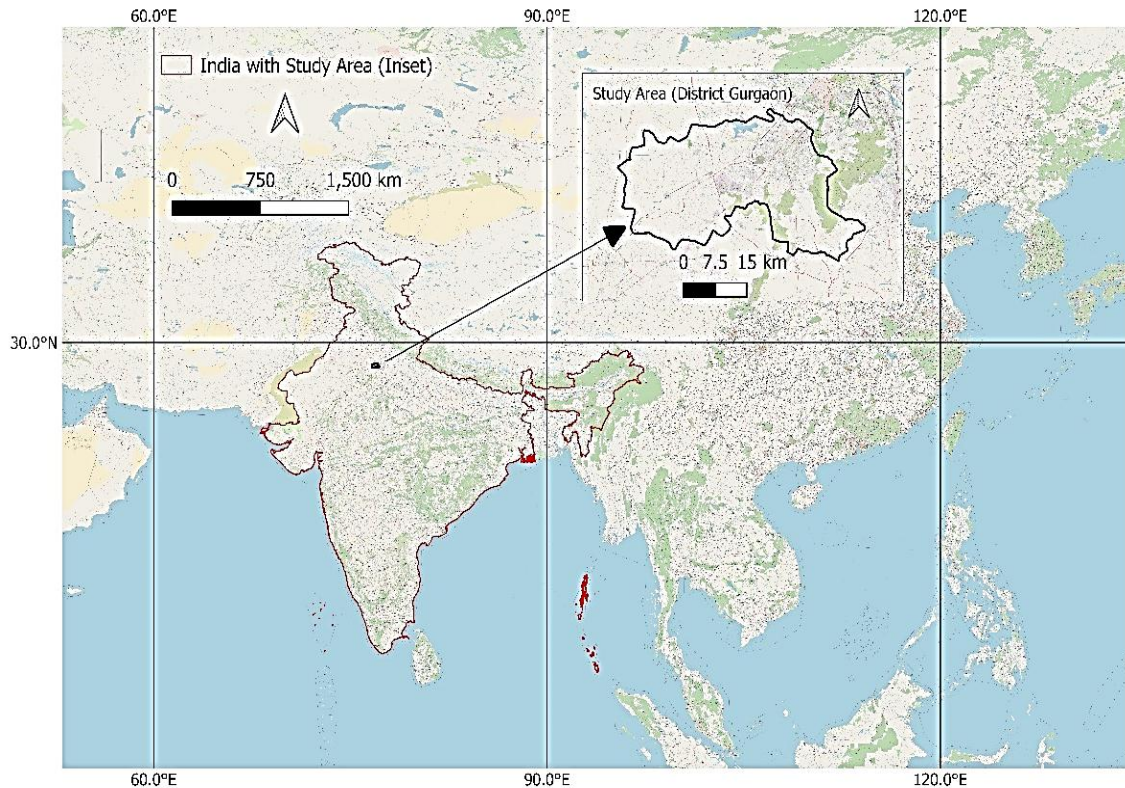
Fig 1. Location Map of the Study Area

Fig 1. highlights the study area (inset) on the map of India. This study area represents broader global trends in urban expansion, particularly in the developing regions where economic growth and population pressures drive significant land-use changes. For example, Kenya in Nairobi experienced rapid urban spread driven by population growth and economic opportunities (Mundia & Aniya, 2005). Similarly, the Pearl River Delta is a globally recognized example of urban-industrial transformation (Seto *et al.,* 2002). In Sao Paulo, urban growth extended into peripheral areas, creating challenges in infrastructure, housing, and green space preservation (Lima & Magaña Rueda, 2018).

This study uses Landsat satellite images for land classification to predict changes after thirty years. A search on Earth Explorer by USGS (USGS, n.d.) identified Landsat images based on (1) acquisition dates (between March to May of 1993 and 2023), (2) Gurgaon district contour as the study area, and (3) less than 5% cloud cover. The satellite scenes have 30-meter spatial resolutions, each covering 900m x 900m land surface with WRS path and row information. Its bands 2, 3, and 4 are in visible spectra blue (0.450 - 0.51 μm), green (0.53 - 0.59 μm), and red (0.64 - 0.67 μm), respectively; band 5 for NIR (0.85 - 0.88 μm), band 6 for SWIR 1 (1.57 - 1.65 μm), band 7 for SWIR 2 (2.11 - 2.29 μm). Various band

combinations are used in the study for false-colored images to display different land cover types required in data validation.

The resulting images with path/row information in Table 1 have minimal time gaps between acquisitions. Geometric corrections applied by USGS using the Dark Object Subtraction (DOS) procedure (Zhang *et al.,* 2010) were available with data.

Table 1. Landsat Scenes Used for LC Classification

#	Landsat Scene Identifier	Acquired	Path	Row	CC*
1	LC81460412023097LGN00	2023-04-07	146	41	0.3
2	LC81470402023104LGN00	2023-04-14	147	40	0.5
3	LT05_L1TP_146040_19930506_20200914_02_T1	1993-05-06	146	40	0
4	LT05_L1TP_17040_19930513_20200914_02_T1	1993-05-13	147	40	0

* Cloud Cover

The relevant two satellite scene pairs (1, 2, and 3, 4) from Table 1 were mosaicked for the study area and then cropped according to a contour to create the region of interest.

RESULTS AND DISCUSSION

The findings highlight the predicted LC changes from 2023 to 2053, presented through maps and statistical summaries. An unsupervised k-means ML model was applied with k = 30, a distance threshold = 0.005, maximum SD = 0.2, and minimum class size = 100, producing 30 clusters. These clusters were subjected to a supervised ML model to reclassify into Land, Forest, Urban, and Water (Wang *et al.,* 2019). The accuracy assessment is done using overall accuracy, user's accuracy, producer's accuracy, and the kappa coefficient. Fig. 2 and Fig. 3 The model generated the Land Classification maps of the study area (district Gurgaon) in 1993 and 2023, respectively.
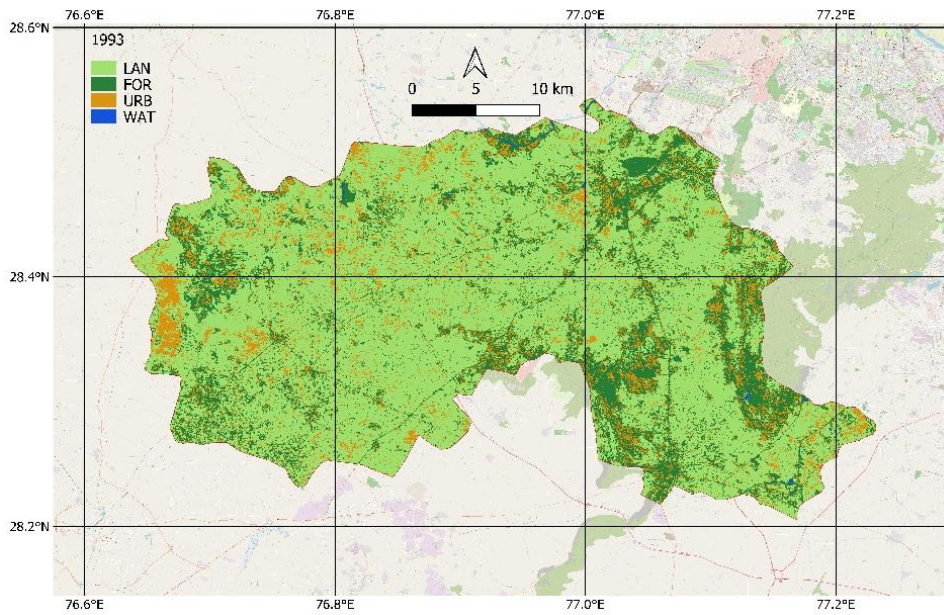
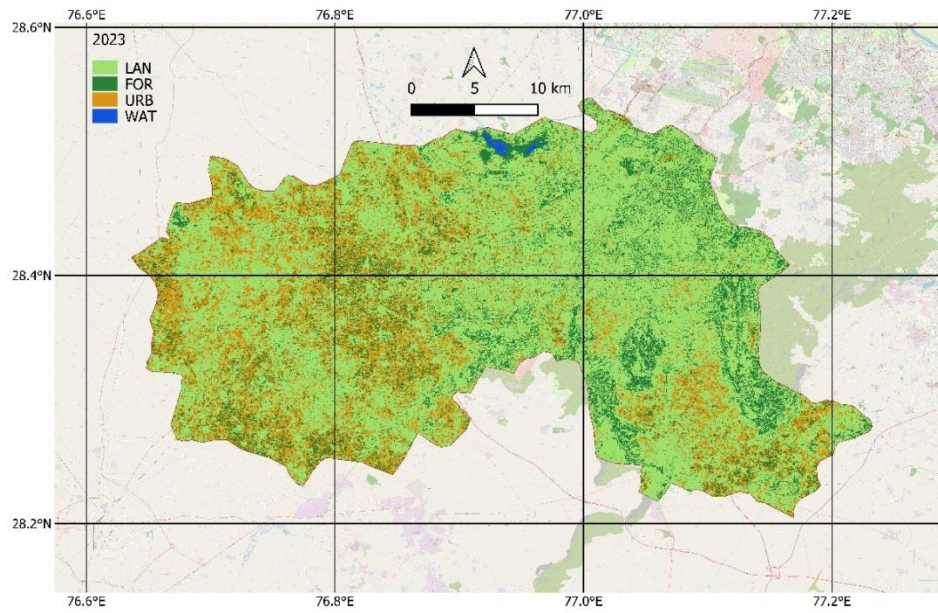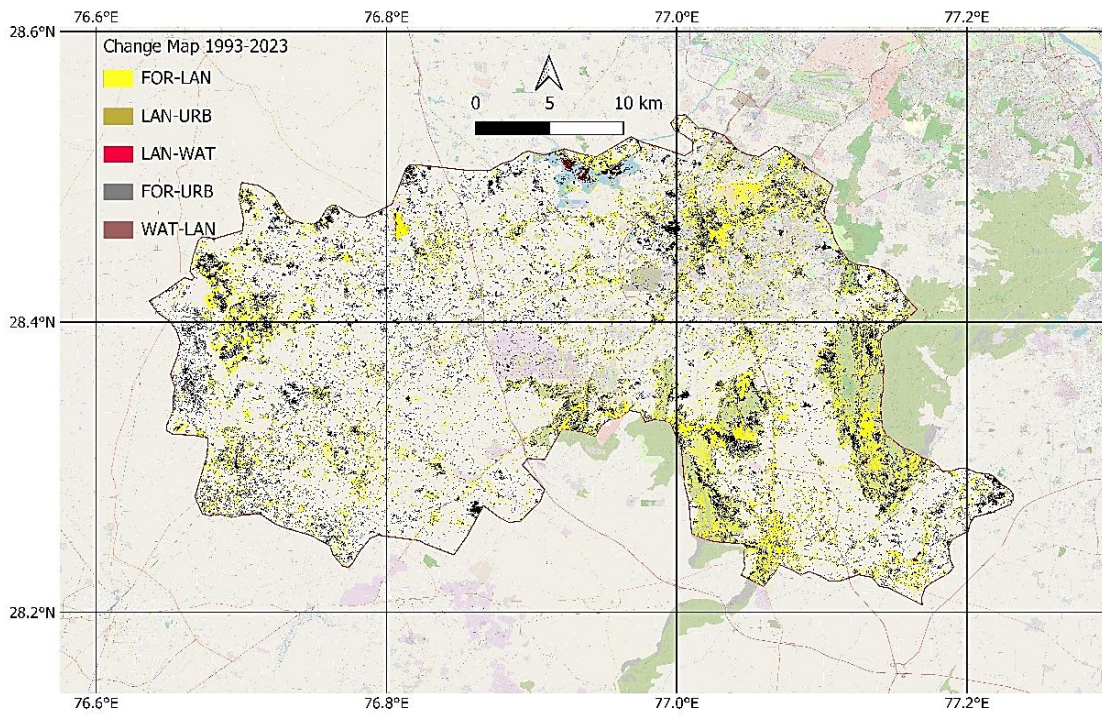**Fig. 2.** Land Classification Map: 1993 (k=4)

Fig. 3. Land Classification Map: 2023 (k=4)

Fig. 4. Land Classification Change Map from 1993 to 2023

Fig. 4 is the change map from 1993 to 2023, which indicates the thirty-year land transformation. The change of information is used to model the simulated map in 2053.

Class statistics

Class statistics is the quantitative measure of each classification (Gondwe *et al.,* 2021). It offers a comprehensive understanding of the current state and dynamics of LC, making them relevant for sustainable development and resource management (Madusanka *et al.,* 2022). The selection of four land classifications can be coarse for applications with finer resolution or granularity. However, they adequately provide consistency in long-term trends and policy-framing goals, supporting informed decisions for sustainable land management and planning.

The detailed class statistics of the study areas are in Table 2 for changes in 1993 and 2023. Land (LAN) decreased from 67.88% in 1993 to 62.21% in 2023, a decline of −5.67% due to the conversion of agricultural land into urban areas or other uses. Forest (FOR) declined from 19.53% in 1993 to 16.26% in 2023, indicating a decrease of 3.26%. The reduction can be attributed to deforestation, urban expansion, and changes in afforestation impacting forest areas. Urban areas had 8.89% rise, growing from 12.47% in 1993 to 21.36% in 2023. Population growth and economic development drove the increase in urban areas. Water Bodies showed a marginal increase, rising from

0.12% in 1993 to 0.16% in 2023. The change is due to improved water management practices, including creating new water bodies or natural fluctuations in water levels.

Table 2. Land Usage percent distributions in 1993 and 2023

Temporal State	Year	LAN (%)	FOR (%)	URB (%)	WAT (%)	Total (%)
Initial (I)	1993	67.88	19.53	12.47	0.12	100
Final (F)	2023	62.21	16.26	21.36	0.16	100
Δ % (F − I)		-5.67	-3.26	8.89	0.04	

State Transition Matrix (STM)

The STM has transition elements (S. K. Singh *et al.,* 2015) outlining the likelihood of one class transitioning to another between successive time intervals. Each cell of the matrix is a class transition probability. Its rows are the initial classes, and the columns represent the final classes after a given interval.

Table 3 is the STM of the study area maps for 1993 and 2023, used to predict the LC map for 2053. The Overall Accuracy (OA) is calculated by summing the diagonal elements (representing no change transitions) and dividing by the total count of observations.

The study, as its novelty, treated specific state transitions in non-diagonal elements as valid transitions. Transitions from FOR to LAN or FOR to URB are valid examples of deforestation to improve the model's accuracy.

Table 3. STM (1993-2023) for Predicting Land Use Changes by 2053

Final 2023	Initial 1993 (→)				
(↓)	LAN (%)	FOR (%)	URB (%)	WAT (%)	Total (%)
TER	41.42	13.51	7.29	0.07	62.28
VEG	9.45	4.10	2.68	0.04	16.26
URB	16.98	1.87	2.44	0.005	21.28
WAT	0.03	0.06	0.07	0.0001	0.16
Total	67.88	19.53	12.47	0.12	100

Final 2023	Initial 1993 (→)				
UA [%]	66.51	25.17	11.45	0.48	
PA [%]	61.02	20.96	19.54	0.65	
OA [%]	81.33				
Kappa	0.64				

* User Accuracy (UA), Producer Accuracy (PA), Overall Accuracy (OA)

Validation

Validation points were randomly selected from the study area to ensure each LC class was adequately represented. These points were compared with Google Maps and corroborated with published data, as shown in Table 4. It includes Government published reports for 2000 and 2008, with the intent to corroborate the trend. The approach has limitations but is a practical alternative to the non-availability of field-based data validation.

Table 4. Year-wise Land Cover Type distribution (%)

Year	Source	LAN (%)	FOR (%)	URB (%)	WAT (%)	Total (%)
1993	Landsat7	67.88	19.53	12.47	0.12	100
2000	* Gov. Report	69.79	18.81	10.92	0.58	100
2008	* Gov. Report	65.57	19.18	15.07	0.16	100
2023	Landsat8	62.21	16.27	21.36	0.16	100

* Gov. Report: Department of Town and Country Planning, Haryana. ((Scott Wilson India Private Limited, 2010))

Accuracy Assessment

Accuracy Assessment ensures models reflect near real-world conditions. It minimizes decision errors to reduce economic and environmental risks. A reliable classification model can be applied to other regions with minimal reconfiguration, ensuring transferability. This study predicts the LC classification map 2053 using the Artificial Neural Network – Multiplayer Perceptron (ANN-MLP) algorithm (Sajan et al., 2022), with parametric values in Table 5. The MOLUSE plug-in of QGIS derived trained data in 1993 and 2023 to simulate trends in 2053, which is essential for understanding and predicting land cover changes.

Table 5. Model Configuration Parameters Used in ANN – MLP

Parameter	Value
Neighborhood (pixel)	1
Learning Rate	0.1
Maximum Iterations	1000
Hidden Layers	10
Momentum	0.05
Number of simulation iterations	5

The configuration parameters are effective in learning, model convergence, and prediction. Neighborhood (pixel) = 1 processes the spectral characteristics of individual pixels. Learning Rate = 0.1 avoids overshooting the optimal solution with stable weight updates during back propagation. Maximum Iterations = 1000 ensures sufficient time for the model to learn the input data patterns and avoid premature termination. Hidden Layers = 10 captures the nonlinear relationships between spectral signatures of land cover classes for extracting higher-order features. Momentum = 0.5 smoothens the optimization process ensuring stability during weight updates without overriding the effect of the learning rate.

The model performance had (1) Overall Accuracy Δ = - 0.00278, (2) Minimum Validation Overall Error = 0.00007, and (3) Kappa = 0.993 to simulate changes in 2053.

Overall accuracy - 0.00278 suggests smaller room for improvement in general. The minimum validation overall error (0.00007) implies prediction accuracy on unseen data. The spatial accuracy assessment used random sampling across all LC classifications to ensure balanced representation. The matrices like kappa (0.993) assessed spatial misclassifications and validated between predicted and reference classifications. Sensitivity analysis was conducted by varying model hyper parameters and evaluating their impact on classification accuracy, ensuring the model is not over-dependent on specific configuration. The minimum validation error (0.00007) indicates that the model generalizes well to unseen data. Table 6 shows the statistical measures between predicted and observed classifications, highlighting trends in urbanization, reduction in forests, and a slight decrease in water coverage.

**Table 6.** Transition Matrix Comparing 2053 with 2023

Final 2053 (↓)	Initial 2023 (→)				
	LAN (%)	FOR (%)	URB (%)	WAT (%)	Total (%)
TER	62.25	0.03	0.0075	0.0021	62.29
VEG	0.01	14.53	0.03	0.0024	14.58
URB	0.007	1.71	21.24	0.0182	22.97
WAT	0.0019	0.001	0.0006	0.13	0.14
Total	62.28	16.26	21.28	0.16	100
UA [%]	99.95	99.77	99.96	98.29	
PA [%]	99.97	89.53	99.96	99.97	
OA	98.25% (Correctly Classified Pixel / Total Pixels)				
Kappa	0.96 (Probability of chance agreement)				

* User Accuracy (UA), Producer Accuracy (PA), Overall Accuracy (OA)

It captures changes predicted after 30 years. It is acknowledged that a finer spatial or temporal detail might be required for localized studies and applications.

The study on a vast area covered has limitations of ground truth data and availability of open-source high-resolution satellite images to substantiate model training and validation data. Fig. 5 is the LC map of the study area of 2053 (simulated). It can provide input to balance the need to preserve natural resources for sustainability.
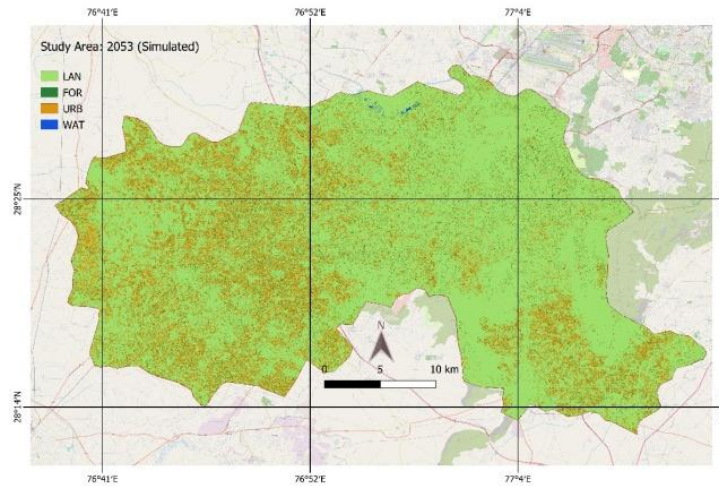
Fig. 5. LC Classification Predicted Map (2053)

An overall change in LAN, implies changes in farming practices or deployment of land management policies aimed at sustainability (Cuong Huu et al., 2023). The decrease in forests highlights concerns about deforestation or conversion of forests to other land uses like urban or agricultural, which affects biodiversity, climate regulation, and ecosystem services (Tilahun et al., 2022). The increase in urban areas, driven by population growth and economic development, brings economic benefits but poses challenges in infrastructure, loss of green spaces, and potential environmental degradation. The reduction in water bodies is minor in absolute terms. Still, it indicates issues in water resource depletion, drying up lakes or rivers, or conversion of water bodies for other land uses. Such a trend will impact water availability and aquatic ecosystems. The encroachment on water reserve areas for agriculture will lead to a decrease in water bodies, indicating a shift towards other land uses (Razali *et al.,* 2018). Fig. 6 (a, b, c, d) shows the percent distribution of LAN, FOR, URB, and WAT over the timeline for 1993, 2008, 2023, and 2053 (simulated).
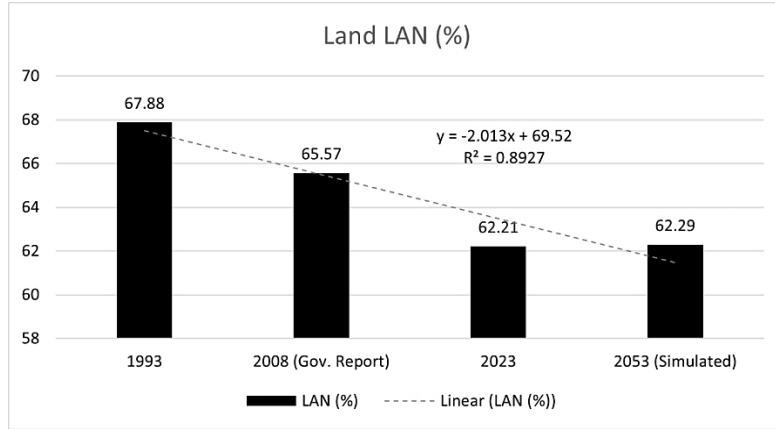
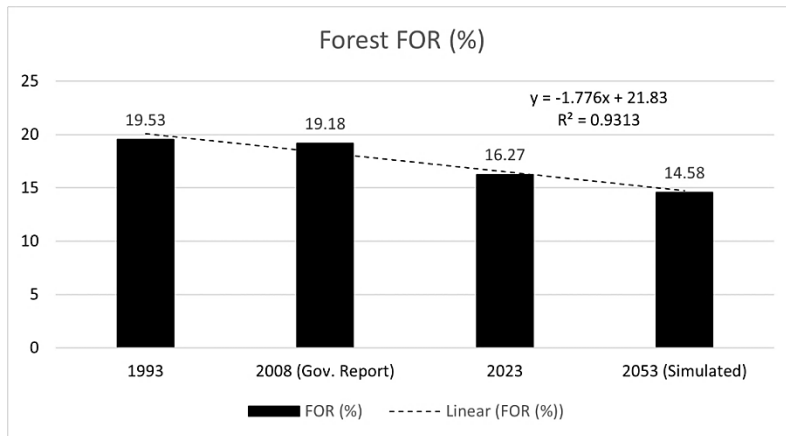**Fig. 6a.** Percentage distribution of LAN

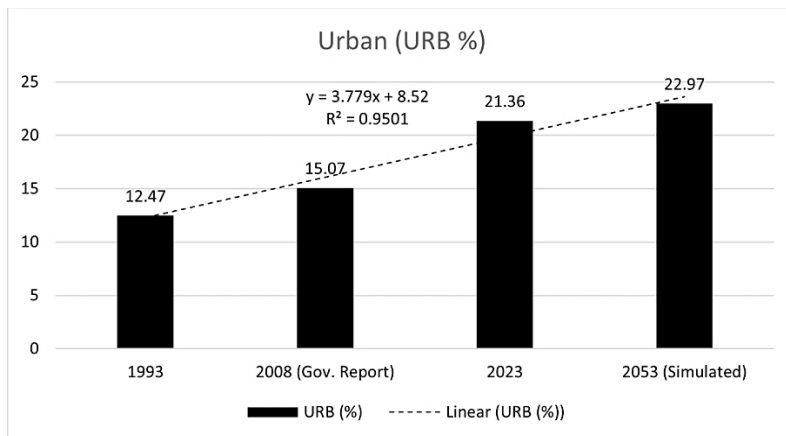**Fig. 6b.** Percentage distribution of FOR

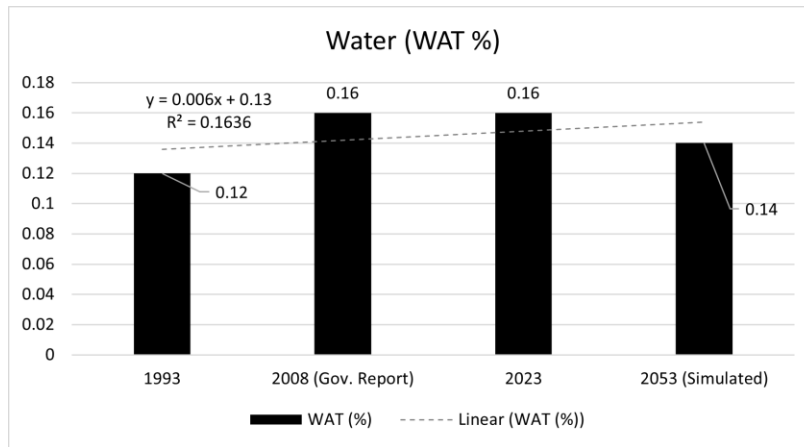**Fig. 6c.** Percentage distribution of URB

Fig. 6d. Percentage distribution of WAT

The dotted trend lines, fitting linear equations, show the overall data pattern and direction, providing insights into long-term trends.

Accuracy assessment has a few challenges. Similar spectral signatures of LC types may cause misclassification, as pixels may contain multiple types, reducing precision (Adhikari et al., 2023). Imbalanced LC classes affect the model accuracy. Imbalanced LC classes occur when some land cover types have more samples than others, leading to biased models (Kumar et al., 2020). Temporal variability due to seasonal changes can alter land cover appearance, leading to misclassification. The referenced data errors in ground truth data can lead to incorrect accuracy assessments. Integrated techniques in ML, feature reduction methods, and high-quality reference data can improve classification precision, leading to more reliable land management decisions.

Socio-economy

Socio-economy growth adds stress on infrastructure, housing, and public services. The loss of vegetation reduces clean air, climate regulation, and groundwater recharge, which increases costs for environmental management. The conversion of land to urban areas will pressurize food security and loss of farmers livelihood. Expanded urban zones increase pollution, reduce green spaces, and create heat islands, leading to biodiversity loss, disrupted ecosystems, and endangered species. Rapid urbanization degrades soil fertility, agricultural productivity, reduced carbon sequestration, and groundwater depletion. Innovative urbanization strategies and land protection policies can minimize the impact of reducing agricultural and forest areas. Financial incentives to farmers can encourage land sustainability. Rainwater harvesting and groundwater recharge integrated to urban planning can promote nature-based solutions to improve water security. Rising urban heat island (UHI) effects have increased local temperatures by

3-5°C, driving higher energy demand for cooling (Taloor *et al.,* 2024). Policies can enforce green roofs, reflective materials, and tree cover in building codes, green belts around cities to regulate temperature. Forest loss threatens biodiversity and endangered species. Policies extended to protect green corridors and implement reforestation programs are essential. Stringent regulations are needed in the Environmental Impact Assessment (EIA) to prevent habitat destruction during urban development. Policymakers must initiate balanced economic growth with ecological sustainability by adopting integrated land-use policies, urban planning reforms, and environmental protection measures (Turner & Ruscher, 1988).

Scalability

Scaling LC models from the study area to broader regions or national and global levels involves several challenges. It has technical limitations, data availability, resource constraints, and alignment with policy frameworks. ML and simulation models become computationally expensive when applied to larger datasets with finer resolution and an extensive area. Such regions may have inconsistent historical and limited ground-truth data and need to explore alternative datasets or crowd-sourced ground-truth data.

With increased data volume, ML processing becomes complex and ineffective. Algorithms like CNN and RF require significant computing power to process high-resolution images for training and analysis (Cavallaro *et al.,* 2015). Managing large datasets will also require high-capacity advanced storage solutions and distributed file systems, adding operational complexity (Burgueño et al., 2023). Parallel computing frameworks (Cavallaro *et al.,* 2015) can ease scalability challenges. Table 7 summarizes key challenges and their impact.

Table 7. Challenges and impact of scalability in LC classification

Challenge	Example	Constraint
High-resolution images require higher memory and processing power.	Processing ~100,000 km² datasets using DL requires 5–10 times more memory (Hashem *et al.,* 2015).	Computational Constraint
DL models require extensive training in high-dimensional data.	A ten times increase in image resolution can increase training time by 8-12 times (Summers *et al.,* 2022).	Algorithmic Complexity

Scalability in cloud-based computing enables efficient processing of large LC datasets. Parallel deep learning speeds up training, reducing computation time by 50-80% for global-scale LC classification. Scalability also increases prediction uncertainties due to sensor noise, missing data spectral variability, and mixing overlapping spectral signatures, which all add classification errors in heterogeneous landscapes (Li *et al.,*

2024). Moreover, a model trained in one region may not perform well in another due to differences in climate, vegetation, and land-use patterns. Future predictions may not account for unforeseen climate events, land-use policies, or socio-economic changes affecting land cover. Scalability challenges and prediction errors can lead to misclassified land types, causing outdated information and unreliable zoning or conservation decisions by policymakers.

Error Margin

Error margins in LC classification accuracy vary based on data resolution, classification methods, and other complexities. Understanding these margins helps to improve model accuracy by selecting classification techniques, training data, and integrating high-resolution images. Table 8 has an error margin in critical areas of LC accuracy assessment.

Table 8. Error Margin of influencing factors in LC classification

Influencing Factors	Impact on	EM
Image resolution (higher resolution reduces error) Number of LC classes (more classes increase complexity) Training data quality (Chen *et al.,* 2022)	OA	±2% to ±10%
Dataset size (larger training sets reduce error) Class proportions (balanced datasets improve stability) (Adhikari *et al.,* 2023)	Kappa	±0.05 to ±0.15
Similar LC reflectance (example: bare soil vs. urban) Sensor resolution (higher resolution reduces spectral overlap) (Li *et al.,* 2024)	Spectral Mixing	±5% to ±15%
Lower resolution increases uncertainty LC heterogeneity (fragmented landscape has higher errors) (Stehman, 2013)	Pixel Resolution	±5% to ±10%

* EM (Error Margin)

The simulated 2053 forecast has uncertainties with an error margin that accounts for influencing it. The expected overall error margin can range between 5-15%, depending on the accuracy of input data and assumptions.

Lesser image resolution helps to identify smaller-scale urbanization and forest areas. Errors in the preprocessing phase and misclassification due to spectral mixing propagate into the model prediction error. Reliability and accuracy thus depend on the data quality used to derive the STM, but its transition probabilities might not account for socio-economic or environmental changes. It also ignores policy interventions or technological advancement. The prediction accuracy declines with increased prediction interval due to a uniform transition rule across the simulation period (Aburas *et al.,* 2017). It is a challenge to implement the interplay of social, human, and economic elements into the simulation results (Jafari *et al.,* 2016).

The validation relies on historical government reports and comparisons with

observed data and satellite images. Any deviation in process, inaccuracies in a report, or human error in observation will impact the reliability of model predictions. Addressing the predicted loss of forests and water bodies should be a priority to ensure ecological balance and long-term sustainability. Urban planning should focus on creating sustainable cities that minimize environmental impacts.

Way Forward

The study witnessed significant land change transformations that can degrade the ecosystems and biodiversity. It invoked an environmental sustainability framework that can analyze the loss of natural habitats, depletion of groundwater resources, and increased pollution levels associated with urbanization and industrialization (Kumar & Singh, 2022). The development processes can address socio-economic disparities and promote inclusive development as a central goal for adopting equitable land use practices in the district.

Collaborating with policymakers is essential to overcome scalability challenges, particularly with government agencies to access administrative datasets, socio-economic statistics, and ground-truthing information. Global organizations like NASA, ESA, USGS, and ISRO can support access to high-quality satellite images for additional study. Private-sector technology firms can support advanced computing infrastructure and innovative solutions.

The study has the potential to integrate advanced modeling techniques with socio-environmental factors and complex data sources to generate impactful predictions in climate change scenarios, including the effects of temperature, precipitation, and drought on land use or climate-sensitive areas like wetlands, mangroves, and biodiversity hotspots. By pursuing advanced research avenues, LC modeling can evolve into a powerful tool for addressing global challenges like climate change, urbanization, and biodiversity loss. These advancements will increase model accuracy and applicability of research findings translated into actionable insights for sustainable land-use planning and policy development. Continued research and development are needed to improve the accuracy and reliability of the simulation models. Advances in this field will lead to improved models that can account for a wide range of external factors in complex systems.

The changed map in 2053 provides early caution to protect the ecosystem, as substantiated by the model's accuracy and reliability in prediction.

ACKNOWLEDGMENTS

FUNDING AND FINANCIAL SUPPORT

CONFLICT OF INTEREST

The authors declare that they have no conflict of interest.

REFERENCES

Aburas, M. M., Ho, Y. M., Ramli, M. F. and Ash'aari, Z. H. 2017. Improving the capability of an integrated CA-Markov model to simulate spatio-temporal urban growth trends using an Analytical Hierarchy Process and Frequency Ratio. *International Journal of Applied Earth Observation and Geoinformation*, **59**: 65–78. https://doi.org/10.1016/j.jag.2017.03.006

Adhikari, A., Menon, H. B. and Lotliker, A. 2023. Coupling of hydrography and bio-optical constituents in a shallow optically complex region using ten years of in-situ data. *ISPRS Journal of Photogrammetry and Remote Sensing*, **202**: 499–511. https://doi.org/10.1016/j.isprsjprs.2023.07.014

Arsanjani, J. J., Kainz, W. and Azadbakht, M. 2011. Monitoring and Spatially Explicit Simulation of Land Use Dynamics: From Cellular Automata to Geosimulation - A Case Study of Tehran, Iran. 2011 *International Symposium on Image and Data Fusion*, 1–4. https://doi.org/10.1109/ISIDF.2011.6024203

Burgueño, A. M., Aldana-Martín, J. F., Vázquez-Pendón, M., Barba-González, C., Jiménez Gómez, Y., García Millán, V. and Navas-Delgado, I. 2023. Scalable approach for high-resolution land cover: A case study in the Mediterranean Basin. *Journal of Big Data*, **10**(1): 91. https://doi.org/10.1186/s40537-023-00770-z

Cavallaro, G., Riedel, M., Bodenstein, C., Glock, P., Richerzhagen, M., Goetz, M. and Benediktsson, J. A. 2015. Scalable developments for big data analytics in remote sensing. 2015 IEEE International Geoscience and Remote Sensing Symposium (IGARSS), 1366–1369. https://doi.org/10.1109/IGARSS.2015.7326030

Chen, M., Niu, J., Li, M., Zhang, L., Ji, Y., Wan, W. and Wu, Q. M. J. 2022. A Motion Compensation Method for Shipborne HFSWR by Using Dual Reference RF Signals Generated Onshore. *Remote Sensing*, **14**(5): 1055. https://doi.org/10.3390/rs14051055

Cuong Huu, N., Cuong Van and Tien My Ngoc. 2023. Monitoring and Modeling of Spatio-Temporal Urban Expansion and Land Use/Land-Cover Change in Mountain Landscape: A Case Study of Dalat City, Vietnam. *Environment and Natural Resources Journal*, **21**(5): 1–15. https://doi.org/10.32526/ennrj/21/20230086

FAO (Ed.). 2016. Forests and agriculture: Land-use challenges and opportunities. FAO.

Gondwe, J. F., Lin, S. and Munthali, R. M. 2021. Analysis of Land Use and Land Cover Changes in Urban Areas Using Remote Sensing: Case of Blantyre City.

Discrete Dynamics in Nature and Society, pp. 1–17. https://doi.org/10.1155/2021/8011565

Hamad, R., Balzter, H. and Kolo, K. 2018. Predicting Land Use/Land Cover Changes Using a CA-Markov Model under Two Different Scenarios. *Sustainability*, **10**(10): 3421. https://doi.org/10.3390/su10103421

Hashem, I. A. T., Yaqoob, I., Anuar, N. B., Mokhtar, S., Gani, A. and Ullah Khan, S. 2015. The rise of "big data" on cloud computing: Review and open research issues. *Information Systems*, **47**: 98–115. https://doi.org/10.1016/j.is.2014.07.006

Jafari, M., Majedi, H., Monavari, S. M., Alesheikh, A. A. and Zarkesh, M. K. 2016. Dynamic simulation of urban expansion through a CA-Markov model Case study: Hyrcanian region, Gilan, Iran. *European Journal of Remote Sensing*, **49**(1): 513–529. https://doi.org/10.5721/EuJRS20164927

Koomen, E. and Borsboom van Beurden, J. A. M. (Eds.). 2011. Land-use modelling in planning practice. Springer.

Kumar, S., Shwetank and Jain, K. 2020. A Multi-Temporal Landsat Data Analysis for Land-use/Land-cover Change in Haridwar Region using Remote Sensing Techniques. *Procedia Computer Science*, **171**: 1184–1193. https://doi.org/10.1016/j.procs.2020.04.127

Kumar, S. and Singh, T. 2022. Study of environmental condition and sustainable solid waste management in Gurugram City. *International Journal of Health Sciences*, 5723–5731. https://doi.org/10.53730/ijhs.v6nS5.9948

Li, Z., Chen, B., Wu, S., Su, M., Chen, J. M. and Xu, B. 2024. Deep learning for urban land use category classification: A review and experimental assessment. *Remote Sensing of Environment*, 311, 114290. https://doi.org/10.1016/j.rse.2024.114290

Lima, G. N. D. and Magaña Rueda, V. O. 2018. The urban growth of the metropolitan area of Sao Paulo and its impact on the climate. *Weather and Climate Extremes*, **21**: 17–26. https://doi.org/10.1016/j.wace.2018.05.002

Madusanka, S., Abenayake, C., Jayasinghe, A. and Perera, C. 2022. A Decision-Making Tool for Urban Planners: A Framework to Model the Interdependency among Land Use, Accessibility, Density, and Surface Runoff in Urban Areas. *Sustainability*, **14**(1): 522. https://doi.org/10.3390/su14010522

Markham, B., Barsi, J., Kvaran, G., Ong, L., Kaita, E., Biggar, S., Czapla-Myers, J., Mishra, N. and Helder, D. 2014. Landsat-8 Operational Land Imager Radiometric Calibration and Stability. *Remote Sensing*, **6**(12): 12275–12308. https://doi.org/10.3390/rs61212275

Mary L. McHugh. 2012. Interrater reliability: The kappa statistic. *Biochemia Medica*, 276–282.

Memarian, H., Kumar Balasundram, S., Bin Talib, J., Teh Boon Sung, C., Mohd Sood, A. and Abbaspour, K. 2012. Validation of CA-Markov for Simulation of Land Use and Cover Change in the Langat Basin, Malaysia. *Journal of Geographic Information System*, **04**(06): 542–554. https://doi.org/10.4236/jgis.2012.46059

Mondal, Md. S., Sharma, N., Garg, P. K. and Kappas, M. 2016. Monitoring and Spatially Explicit Simulation of Land Use Dynamics: From Cellular Automata to Geosimulation—A Case Study of Tehran, Iran. *The Egyptian Journal of Remote Sensing and Space Science*, **19**(2): 259–272. https://doi.org/10.1016/j.ejrs.2016.08.001

Mundia, C. N. and Aniya, M. 2005. Analysis of land use/cover changes and urban expansion of Nairobi city using remote sensing and GIS. *International Journal of Remote Sensing*, **26**(13): 2831–2849. https://doi.org/10.1080/01431160500117865

Pontius, R. G. and Schneider, L. C. 2001. Land-cover change model validation by an ROC method for the Ipswich watershed, Massachusetts, USA. *Agriculture, Ecosystems & Environment*, **85**(1–3), 239–248.

https://doi.org/10.1016/S0167-8809(01)00187-6

Qiu, H., Zhang, J., Han, H., Cheng, X. and Kang, F. 2023. Study on the impact of vegetation change on ecosystem services in the Loess Plateau, China. *Ecological Indicators*, **154**: 110812. https://doi.org/10.1016/j.ecolind.2023.110812

Razali, A., Syed Ismail, S. N., Awang, S., Praveena, S. M. and Zainal Abidin, E. 2018. Land use change in highland area and its impact on river water quality: A review of case studies in Malaysia. *Ecological Processes*, **7**(1): 19. https://doi.org/10.1186/s13717-018-0126-8

Sajan, B., Mishra, V. N., Kanga, S., Meraj, G., Singh, S. K. and Kumar, P. 2022. Cellular Automata-Based Artificial Neural Network Model for Assessing Past, Present, and Future Land Use/Land Cover Dynamics. **Agronomy**, **12**(11): 2772. https://doi.org/10.3390/agronomy12112772

Scott Wilson India Private Limited. 2010, September. Preparation of Sub Regional Plan for Haryana Sub-Region of NCR-2021. Department of Town and Country Planning, Haryana. https://www.smsfoundation.org/wp-content/themes/sehgal/pdf/Draft%20Final%20Report-Haryana%20Sub-Regional%20Plan%202021.pdf

Seto, K. C., Kaufmann, R. K. and Woodcock, C. E. 2002. Monitoring Land Use Change in the Pearl River Delta, China.

In S. J. Walsh & K. A. Crews-Meyer (Eds.), Linking People, Place, and Policy (pp. 69–90). Springer US. https://doi.org/10.1007/978-1-4615-0985-1_4

Singh, S. and Biswas, R. 2022. Analysis of Land Use Change Effects/Impacts on Surface Water Resources in Delhi. *Urban Science*, **6**(4): 92. https://doi.org/10.3390/urbansci6040092

Singh, S. K., Mustak, Sk., Srivastava, P. K., Szabó, S. and Islam, T. 2015. Predicting Spatial and Decadal LULC Changes Through Cellular Automata Markov Chain Models Using Earth Observation Datasets and Geo-information. *Environmental Processes*, **2**(1): 61–78. https://doi.org/10.1007/s40710-015-0062-x

Stehman, S. V. 2013. Estimating area from an accuracy assessment error matrix. *Remote Sensing of Environment*, **132**: 202–211. https://doi.org/10.1016/j.rse.2013.01.016

Subedi, P., Subedi, K. and Thapa, B. 2013. Application of a Hybrid Cellular Automaton – Markov (CA-Markov) Model in Land-Use Change Prediction: A Case Study of Saddle Creek Drainage Basin, Florida. *Applied Ecology and Environmental Sciences*, 1(6): 126–132. https://doi.org/10.12691/aees-1-6-5

Summers, N., Johnsen, G., Mogstad, A., Løvås, H., Fragoso, G. and Berge, J. 2022. Underwater Hyperspectral Imaging of Arctic Macroalgal Habitats during the Polar Night Using a Novel Mini-ROV-UHI Portable System. **Remote Sensing**, **14**(6): 1325. https://doi.org/10.3390/rs14061325

Taloor, A. K., Sharma, S., Parsad, G. and Jasrotia, R. 2024. Land use land cover simulations using integrated CA-Markov model in the Tawi Basin of Jammu and Kashmir India. *Geosystems and Geoenvironment*, **3**(2): 100268. https://doi.org/10.1016/j.geogeo.2024.100268

Tilahun, D., Gashu, K. and Shiferaw, G. T. 2022. Effects of Agricultural Land and Urban Expansion on Peri-Urban Forest Degradation and Implications on Sustainable Environmental Management in Southern Ethiopia. *Sustainability*, **14**(24): 16527. https://doi.org/10.3390/su142416527

Tokihiro, T., Takahashi, D., Matsukidaira, J. and Satsuma, J. 1996. From Soliton Equations to Integrable Cellular Automata through a Limiting Procedure. *Physical Review Letters*, **76**(18), 3247–3250. https://doi.org/10.1103/PhysRevLett.76.3247

Turner, M. G. and Ruscher, C. L. 1988. Changes in landscape patterns in Georgia, USA. *Landscape Ecology*, **1**(4): 241–251. https://doi.org/10.1007/BF00157696

USGS. (n.d.). EarthExplorer—USGS. https://earthexplorer.usgs.gov/

Wang, M., Cai, L., Xu, H. and Zhao, S. 2019. Predicting land use changes in northern China using logistic regression, cellular automata, and a Markov model. *Arabian Journal of Geosciences*, **12**(24): 790. https://doi.org/10.1007/s12517-019-4985-9

Zhang, Z., He, G. and Wang, X. 2010. A practical DOS model-based atmospheric correction algorithm. *International Journal of Remote Sensing*, **31**(11): 2837–2852. https://doi.org/10.1080/01431160903124682